**Liquid Crystals**
Publication details, including instructions for authors and subscription information:
http://www.informaworld.com/smpp/title~content=t713926090

# Coupling of liquid crystalline and polymer network properties in LC-elastomers

M. Brehmer[a]; R. Zentel[a]; F. Gießbtelmann[b]; R. Germer[b]; P. Zugenmaier[b]
[a] Institut für Organische Chemie, Universität Mainz, Mainz, Germany [b] Institut für Physikalische Chemie, Technische Universität Clausthal, Clausthal-Zellerfeld, Germany

**To cite this Article** Brehmer, M. , Zentel, R. , Gießbtelmann, F. , Germer, R. and Zugenmaier, P.(1996) 'Coupling of liquid crystalline and polymer network properties in LC-elastomers', Liquid Crystals, 21: 4, 589 — 596
**To link to this Article: DOI:** 10.1080/02678299608032868
**URL:** http://dx.doi.org/10.1080/02678299608032868

LIQUID CRYSTALS, 1996, VOL. 21, NO. 4, 589–596

# Coupling of liquid crystalline and polymer network properties in LC-elastomers

by M. BREHMER, R. ZENTEL*
Institut für Organische Chemie, Universität Mainz, J. J.-Becher-Weg 18-20,
D-55099 Mainz, Germany

F. GIEßELMANN*, R. GERMER and P. ZUGENMAIER
Institut für Physikalische Chemie, Technische Universität Clausthal,
Arnold-Sommerfeld-Str. 4, D-38678 Clausthal-Zellerfeld, Germany

(*Received 15 September 1995; in final form 16 May 1996; accepted 12 June 1996*)

Electromechanical and electro-optical properties which result from an interplay of ferroelectricity and elasticity in slightly crosslinked ferroelectric liquid crystalline elastomers are studied in the vicinity of the smectic C*–smectic A* phase transition. In the chiral smectic C* phase, the formation of the network during the crosslinking procedure stabilizes the polar orientation which is present. On heating the smectic C* network into the chiral smectic A* phase, an induced tilt is observed (mechanoclinic effect). The internal mechanical stress induced by the network formation appears to act like an external electric bias-voltage. The results are discussed in terms of a simple Landau model.

## 1. Introduction

Polymer networks, in general, retain memory about their state (e.g. swelling and orientation) during crosslinking [1]. Since the polymer chains of liquid crystalline (LC) polymers adopt an anisotropic conformation in the liquid crystalline state [2], this memory of the network is transferred to the LC phase. This leads to a permanent conservation of the LC orientation which is present during crosslinking, as long as the elastomer is not deformed [3–6]. A reorientation of the LC director—keeping the macroscopic shape of the network unchanged—leads therefore to elastic counter forces (see figure 1). For this reason a switching of macroscopically fixed nematic elastomers in electric fields has never been observed (only a partial director reorientation was observed in freely floating LC elastomer particles, where it was accompanied by a shape variation [7, 8]).

In ferroelectric LC elastomers with ferroelectric LC phases, the coupling between the external field and the polar axis is however much stronger, and electric field induced switching might be expected. Recently we were able to prepare slightly crosslinked ferroelectric LC elastomers, which allow ferroelectric-like switching in an electric field (see figure 1) [9, 10]. In these systems, only one polar state is stable without an external electric field (this is the polar state present during crosslinking). It is, however, possible to reach the second switching state by electrical fields of opposite voltage.

We are still far from understanding the physics of these systems in detail [11]. However, we have made some experiments which improve our knowledge of the coupling between the polymer network, the LC director and the spontaneous polarization in these networks.

## 2. Experimental

The synthesis of the crosslinkable polymer **1** (see the scheme) and its photocrosslinking have been described previously [10]. The key steps of the crosslinking are the orientation of the uncrosslinked polymer **1**, containing a photoinitiator, in a commercially available EHC-cell (electrode area 0·16 mm$^2$, electrode separation 10 μm), and the photocrosslinking in the chiral smectic C* phase under a static electric field of 200 V [10]. The characterization of the elastomers was carried out using a polarizing microscope equipped with a photodiode and a Mettler hot stage. Optical response and applied voltage were registered on a storage oscilloscope according to the procedure described in refs. [10, 12]. For the measurement of the polarization and the tilt angle, a cell with an electrode gap of 4 μm was used.

## 3. Electromechanical coupling

While the transition between the chiral smectic C* and the chiral smectic A* phase can be easily detected

---

*Author for correspondence.

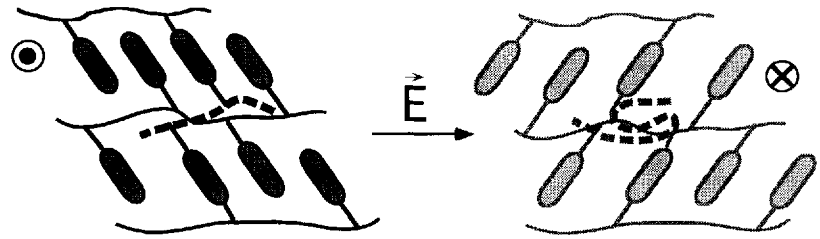

Figure 1. Switching of a ferroelectric LC elastomer leads to deformation of the network.

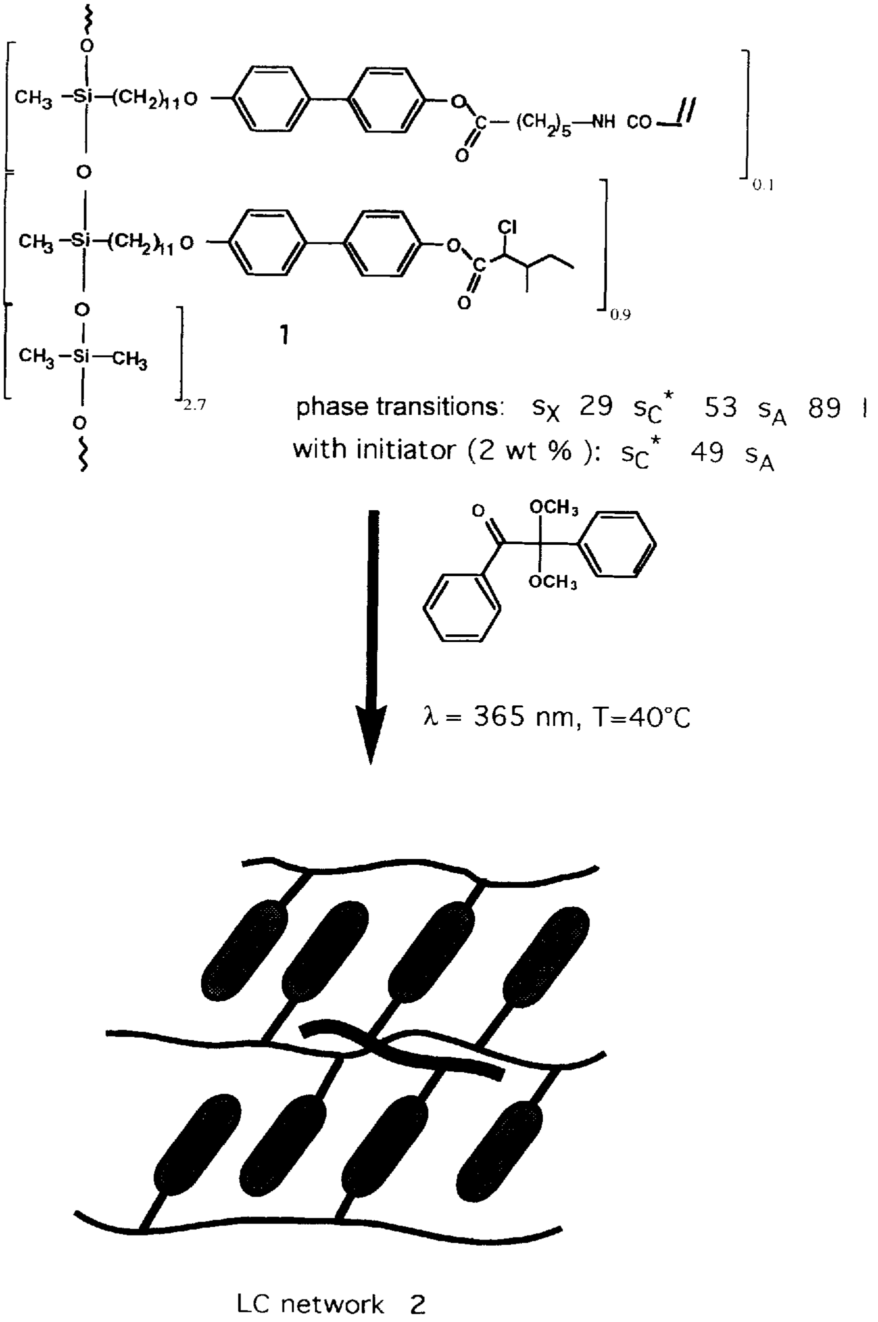

Scheme. Photocrosslinking of the ferroelectric LC polysiloxane **1** leads to LC elastomer **2** for the uncrosslinked polymer **1** (texture observations and switching studies), this is no longer the case for the crosslinked elastomer **2**. The elastomer **2** does not show any texture change because the crosslinking freezes the director; whereas a transition between a fan-shaped and a broken fan-shaped texture can be observed for polymer **1**. The long switching times of elastomer **2** (seconds) make any determination of the spontaneous polarization of the crosslinked polymer impossible. To overcome these problems we analysed the temperature dependence of the optical hysteresis (figure 2), which allows a significant characterization of the crosslinking effect through the following observations:

(a) The midpoint of the ferroelectric hysteresis of the smectic C* network is shifted away from zero voltage (cf. figure 2(*a*)), corresponding to the stabilization of the ferroelectric state which was present during the crosslinking procedure.

(b) The hysteresis becomes narrower with increasing temperature and disappears at about 49–50°C, indicating the ferroelectric (smectic C*) to paraelectric (smectic A*) transition.

(c) Above 49°C, only a (non-linear) electroclinic response is observed (figure 2(*b*)). All curves in figure 2(*b*) intersect at a non-zero voltage. For zero voltage a finite tilt is observed for the smectic A* phase.

In principle, either the shift of the ferroelectric smectic C* hysteresis or the non-zero tilt of the smectic A* phase may be compensated by an external bias-voltage. This consideration shows that the internal mechanical stress introduced by the crosslinking effect

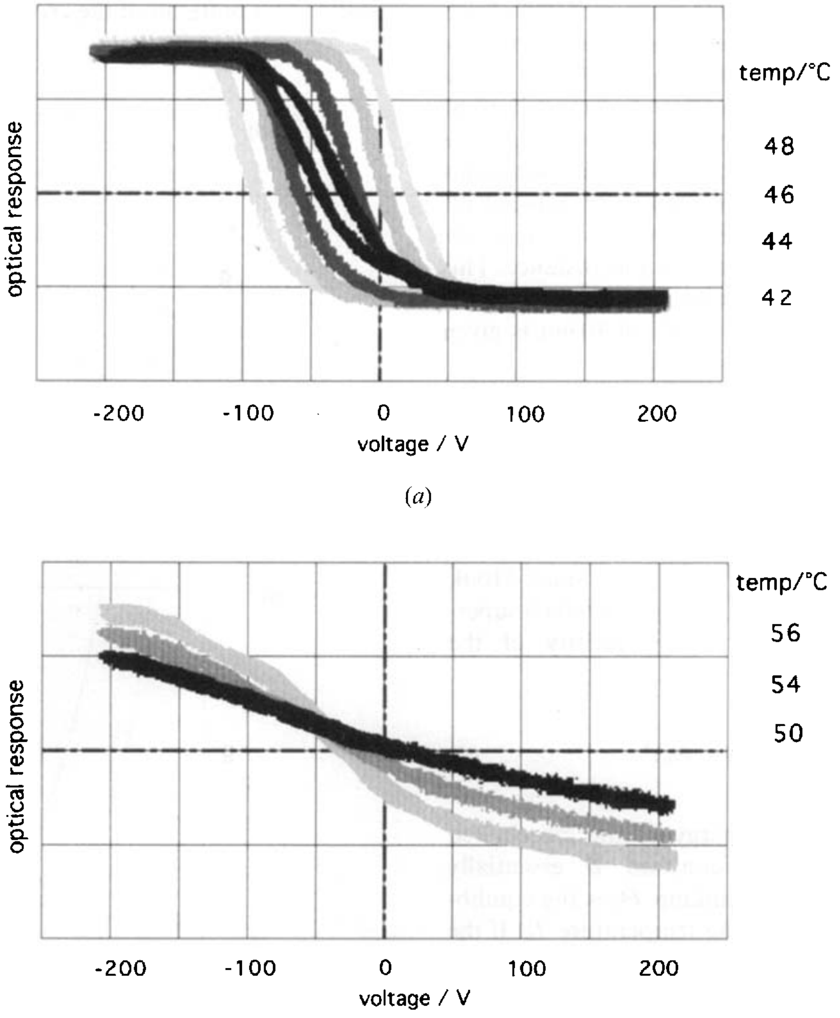

Figure 2. Temperature dependence of the optical hysteresis of LC elastomer **2** ($S_C^*49S_A^*$). (*a*) Ferroelectric behaviour of the $S_C^*$ phase (42, 44, 46 and 48°C, respectively); (*b*) electroclinic behaviour of the $S_A^*$ phase (50, 54 and 56°C, respectively).

formally acts like an external bias voltage in the opposite direction. This analogy also includes the electroclinic effect. An electric field applied to a chiral smectic A* phase induces a finite director tilt (electroclinic effect). In our case a finite smectic A* tilt is induced in the absence of an electric field by the internal mechanical stress within the crosslinked system. Therefore it is convenient to denote this effect as 'mechanoclinic' effect.

In this context is is interesting to discuss whether the tilt induced in the smectic A phase by the network is homogenous throughout the phase, or whether it is pinned to the vicinity of the crosslinked points (netpoints). In order to answer this question, the average distance between the crosslinked points has to be compared to the lateral wavelength of the soft mode (i.e. the lateral correlation length of the induced tilt). Before crosslinking, polymer **1** was characterized by GPC. These measurements showed it to have the same dimensions as polystyrene of molecular mass of 20 000. Such a polystyrene has (depending on the solvent) an end-to-end length of the polymer chain of 5–10 nm. Since elastomer **2** was completely crosslinked, it must have at least two crosslinked points per polymer chain. Therefore the average distance between the crosslinked points has to be less than 5–10 nm. The mechanically induced tilt can therefore be considered as homogenous if the wavelength of the soft mode is larger than this distance. This has been shown to be true, at least in the vicinity of the phase transition (a correlation length of 10 nm is given in ref. [13]).

The phase transition temperature observed for the crosslinked system (see point (b) above) is nearly unchanged compared with that of the uncrosslinked polymer. This observation shows that the crosslinking effect may be considered to cause only a small disturbance of the basic thermodynamic functions. This allows us to separate the crosslinking effect by a small Hook elastic energy term $V = 1/2 \times D \times (\Theta - \Theta_0)^2$ which superimposes on the Gibbs free energy density of the uncrosslinked system.

$$g_{\mathrm{cl}} = g + \frac{1}{2} D(\Theta - \Theta_0)^2 \qquad (1)$$

where $g_{\mathrm{cl}}$ is the Gibbs free energy of the crosslinked polymer. The Hook elastic constant $D$ essentially depends on the degree of crosslinking. $\Theta_0$ is the equilibrium tilt angle at the crosslinking temperature $T_0$. If the tilt angle $\Theta$ changes from $\Theta_0$ at temperatures $T \neq T_0$ or by application of an external electric field, a mechanical torque $-D(\Theta - \Theta_0)$ arises which tries to preserve the crosslinking tilt $\Theta_0$ and leads to an internal mechanical stress.

The macroscopic effects of this stress are discussed in figure 3. In the absence of external force fields the potential $g$ of the undisturbed smectic C* phase is an even function of $\Theta$ with two minima $\pm\Theta$ representing the ferroelectric switching states (dashed line, figure 3 (*a*). If the elastic function $1/2D(\Theta - \Theta_0)^2$, $\Theta_0 \neq \Theta$ (dotted line, figure 3 (*a*)), is added, the energetic equivalence of the two minima is broken and the ferroelectric state next to $\Theta_0$ is stabilized with respect to the other state (solid line, figure 3 (*a*)). This consideration explains the observation described in point (a) above and leads to a shift of the hysteresis along the $E$-axis. The discriminated state might even vanish, depending on the magnitude of $D$. The potential of an undisturbed (uncrosslinked) smectic A* phase in the absence of an external field is given as function of the tilt $\Theta$ by an even function with a single minimum at $\Theta = \Theta_0$ (dashed line, figure 3 (*b*)). If the same elastic function (dotted line, figure 3 (*b*)) is added, the minimum of the resulting potential becomes shifted to a finite tilt of the crosslinked smectic A* phase.

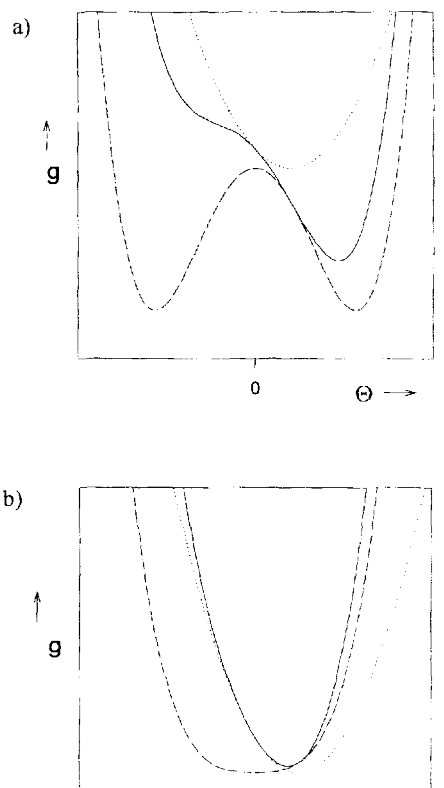

Figure 3. Effect of the network force on the free energy density; (— — ) potential of the undisturbed phase according to equation (8), (...) force due to the network $D = 10\,\mathrm{kJ\,m^{-3}}$ ($\Theta_0 = 10°$), (——) superposition of both. (*a*) $S_C^*$ phase; (*b*) $S_A^*$ phase.

This consideration is related to the observation described in point (c) and explains the occurrence of the mechanoclinic effect.

## 4. Mean field coefficients

In order to quantify our considerations and estimate the magnitude of $D$ from the effects observed, the potential $g$ of the uncrosslinked polymer **1** has to be determined. As a result of the generalized mean field theory by Žekš [14], the energy density of a helically unwound smectic C* phase in an electric field $E$ is given by a Landau-type expansion of the tilt $\Theta$ and the polarization $\mathbf{P}$:

$$g=\frac{1}{2}\alpha(T-T_c)\Theta^2+\frac{1}{4}b\Theta^4+\frac{1}{6}c\Theta^6+\frac{1}{2\chi}\mathbf{P}^2 -CP\Theta-\frac{1}{2}\Omega\mathbf{P}^2\Theta^2-\mathbf{PE} \qquad (2)$$

Besides the order parameters $(\Theta, \mathbf{P})$ and the variables of the state $(T, \mathbf{E})$, equation (2) involves seven material parameters which are the Landau coefficients $\alpha$, $b$ and $c$, the electric susceptibility $\chi$, and the bilinear and biquadratic coupling coefficients $C$ and $\Omega$, respectively. The transition temperature $T_c$ enters into the expansion as the smectic C–smectic A* phase transition temperature of the achiral system (e.g. the same polymer with racemic composition). The transition temperature $T_c^*$ of the chiral polymer actually observed in the experiments is related to $T_c$ by [15]:

$$T_c^*=T_c+\frac{\chi C^2}{\alpha} \qquad (3)$$

The seven material parameters $(\alpha, b, c, \chi, C, \Omega, T_c)$ are available by a careful evaluation of temperature and electric field dependent tilt and polarization data. The experimental techniques and the evaluation procedure leading to the mean field parameters are outlined in detail in refs. [12] and [16]. In this context only a brief summary need be given as follows. For a certain temperature $T$, the director tilt $\Theta$ is measured electro-optically at various electric field strengths $\mathbf{E}$. Simultaneously, the polarization $\mathbf{P}$, which is the sum of the spontaneous polarization $P_s$ and the induced polarization $P_{\text{ind}}$, is recorded by a slight variation of the triangular wave technique [12]. These measurements are repeated for various temperatures in the vicinity of the smectic C*–smectic A* transition and supply experimental data on the functions of state $\Theta(T, E)$ and $P(\Theta, E)$. These data are analysed in terms of the Landau expansion (2). Starting with equation (2) we obtain the equilibrium value of the total polarization $\mathbf{P}$:

$$\mathbf{P}(\Theta,\mathbf{E})=\frac{C\Theta+\mathbf{E}}{\dfrac{1}{\chi}-\Omega\Theta^2} \qquad (4)$$

Replacing $\mathbf{P}$ in equation (2) by expression (4), the Landau expansion reads:

$$g=\frac{1}{2}\alpha(T-T_c)\Theta^2+\frac{1}{4}b\Theta^4+\frac{1}{6}c\Theta^6-\frac{1}{2}\frac{C\Theta+\mathbf{E}^2}{\dfrac{1}{\chi}-\Omega\Theta^2} \qquad (5)$$

Using the equilibrium condition $(\partial g/\partial\Theta)=0$, we obtain

$$T=T_c-\frac{1}{\alpha\Theta}\left[b\Theta^3+c\Theta^5+C\frac{C\Theta+\mathbf{E}}{\dfrac{1}{\chi}-\Omega\Theta^2} -\Omega\Theta\left(\frac{C\Theta+\mathbf{E}}{\dfrac{1}{\chi}-\Omega\Theta^2}\right)^2\right] \qquad (6)$$

which describes the tilt angle $\Theta$ as function of $T$ and $\mathbf{E}$. Equation (6) is a 5th order polynomial of $\Theta$ which cannot be resolved to $\Theta(T, \mathbf{E})$. Therefore we must change the independent variables and obtain $T(\Theta, \mathbf{E})$ instead of $\Theta(T, \mathbf{E})$:

$$T=T_c-\frac{1}{\alpha\Theta}\left[b\Theta^3+c\Theta^5+C\frac{C\Theta+\mathbf{E}}{\dfrac{1}{\chi}-\Omega\Theta^2} -\Omega\Theta\left(\frac{C\Theta+\mathbf{E}}{\dfrac{1}{\chi}-\Omega\Theta^2}\right)^2\right] \qquad (7)$$

Equations (4) and (7) directly allow an analysis of our experimental data. The three parameters $\chi$, $C$, and $\Omega$ are obtained from a fit of the experimental $\mathbf{P}(\Theta, \mathbf{E})$ data with equation (4) (see figure 4 and the table). The other

Table. Summary of Landau coefficients; the accuracy is better than 10% ($\alpha$), better than 20% ($b$), and in the range of the order of magnitude shown ($c$).

| $\alpha$ /kJ m$^{-3}$ K$^{-1}$ | $b$ /kJ m$^{-3}$ | $c$ /kJ m$^{-3}$ | $T_c$ /K | $\chi_r$ | $C$ /V m$^{-1}$ | $\Omega$ V m C$^{-1}$ |
|---|---|---|---|---|---|---|
| 13·3 | 395·5 | 1549 | 330·2 | 2·2 | 46·81 × 10$^6$ | 9·079 × 10$^9$ |

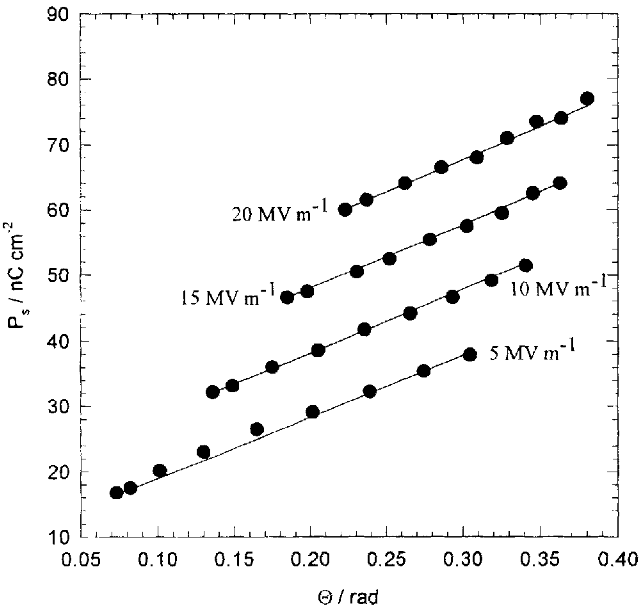

Figure 4. Temperature and field dependence of the spontaneous polarisation. The solid lines represent the best fits according to equation (4).

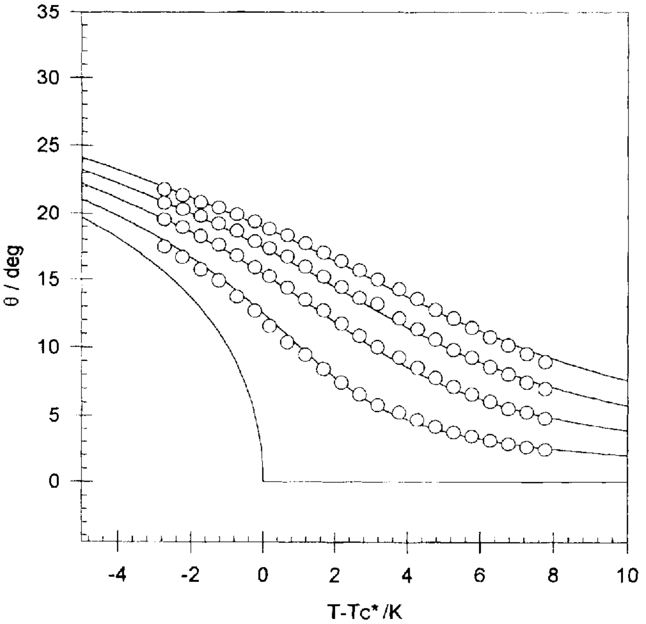

Figure 5. Temperature dependence of the tilt angle and the effect of an applied field. The solid line represents the best fit according to equation (8).

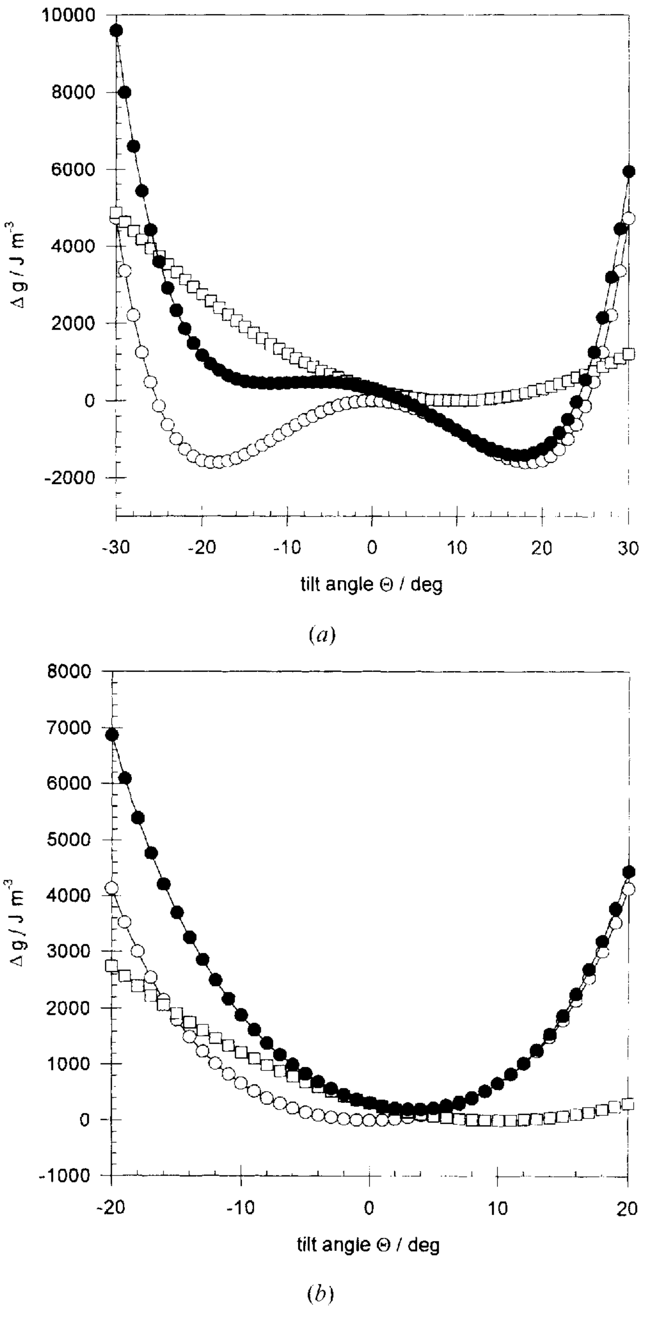

(*a*)

(*b*)

Figure 6. Effect of the network force on the free energy density; (○) calculated potential according to equation (8), (□) force due to the network $D = 10\,\mathrm{kJ\,m^{-3}}$ ($\Theta_0 = 10°$), (●) superposition of both. (*a*) 2 K below the phase transition, $S_C^*$ phase; (*b*) 2 K above the phase transition, $S_A^*$ phase.

parameters $\alpha$, $b$, $c$ and $T_c$ are available from a fit of the experimental $\Theta(T, \mathbf{E})$ data according to equation (7) (see figure 5 and the table) with values of $\chi$, $C$, and $\Omega$ from the first fit. A comparison of fit and experimental data clearly shows that the generalized Landau expansion (2) gives a consistent and high quality description of our system.

The phase transition temperature $T_c^* = T_c$

$+3{\cdot}2\,\mathrm{K} = 330{\cdot}8\,\mathrm{K}$, as obtained from equation (3) and values listed in the table, also agrees well with experimental observations.

Using the parameters listed in the table, we calculated the potential $g(\Theta)$ of the uncrosslinked polymer by equation (5) with $\mathbf{E} = 0$ for $T - T_c = -2\,\mathrm{K}$ (smectic C* phase, open circles in figure 6(*a*)) and $T - T_c = +2\,\mathrm{K}$ (smectic A* phase, open circles in figure 6(*b*)). Adding a Hook elastic potential (open squares in figures 6(*a*) and 6(*b*)) with $D = 10\,000\,\mathrm{kJ\,m^{-3}}$ and $\Theta_0 = 10°$, the potential of the crosslinked system $g_{cl}$ (closed circles in figures 6(*a*) and 6(*b*)) results in a considerable stabilization of one switching state (smectic C* phase, closed circles in figure 6(*a*)) and in a minimum potential at a finite tilt at about 1·5° for the smectic A* state (closed circles in figure 6(*b*)). Roughly speaking, the network specific parameter $D$ should have a magnitude of about $10^4\,\mathrm{J\,m^{-3}}$, leading to $D \approx \alpha(T - T_c)$ if macroscopic effects of the network are observed.

## 5. Electroclinic and mechanoclinic effect

Due to the smectic A* tilt induced by the mechanoclinic effect, a piezo responde $d_{33}$ was observed for the smectic A* phase of our polymer (see figure 7) and also figure 12 in ref. [10]). The piezo effect is closely related to the electroclinic effect, which refers to the tilt $\delta\Theta$ induced by an electric field $\mathbf{E}$.

$$\delta\Theta = \Theta(\mathbf{E}) - \Theta_0(\mathbf{E} = 0) \qquad (8)$$

The electroclinic effect of our polymer is clearly visible in figure 5, showing a strong field dependence of the tilt $\Theta(\mathbf{E})$. The director tilt at zero field $\Theta_0$ was calculated from our experimental data with the mean field coefficients listed in the table and application of equation (7) with $\mathbf{E} = 0$. The results are plotted in figure 5 as a solid line (without experimental points) and serve for the calculation of $\delta\Theta$ which is plotted versus temperature $T$ in figure 8. Figure 8 nicely reflects the soft mode behaviour of the electroclinic effect. Compared with low molar mass ferroelectric liquid crystals, the electroclinic effect is rather high, reaching values of about 18°. This behaviour is related to the low value of the Landau coefficient $\alpha \approx 13\,000\,\mathrm{J\,m^{-3}\,K^{-1}}$ which is about one third of typical values observed for low molar mass ferroelectric liquid crystals [12]! Figure 9 shows the electroclinic effect plotted in a reciprocal representation. The linear dependence of the electroclinic effect compares with the piezo response data (figure 7(*b*)) and reflects the close relation between the mechanoclinic and electroclinic effects. The exact relation between the two effects is still unclear and will be a subject of further investigation.

## 6. Conclusion

Crosslinking of FLC polymers leads to an interesting modification of their mechanical, optical, and electrical properties. The modification is basically described by a network elastic constant $D$, which is controlled by the crosslinking conditions. An improved understanding of the basic physics and chemistry of these systems should lead to functional polymers with defined electromechan-

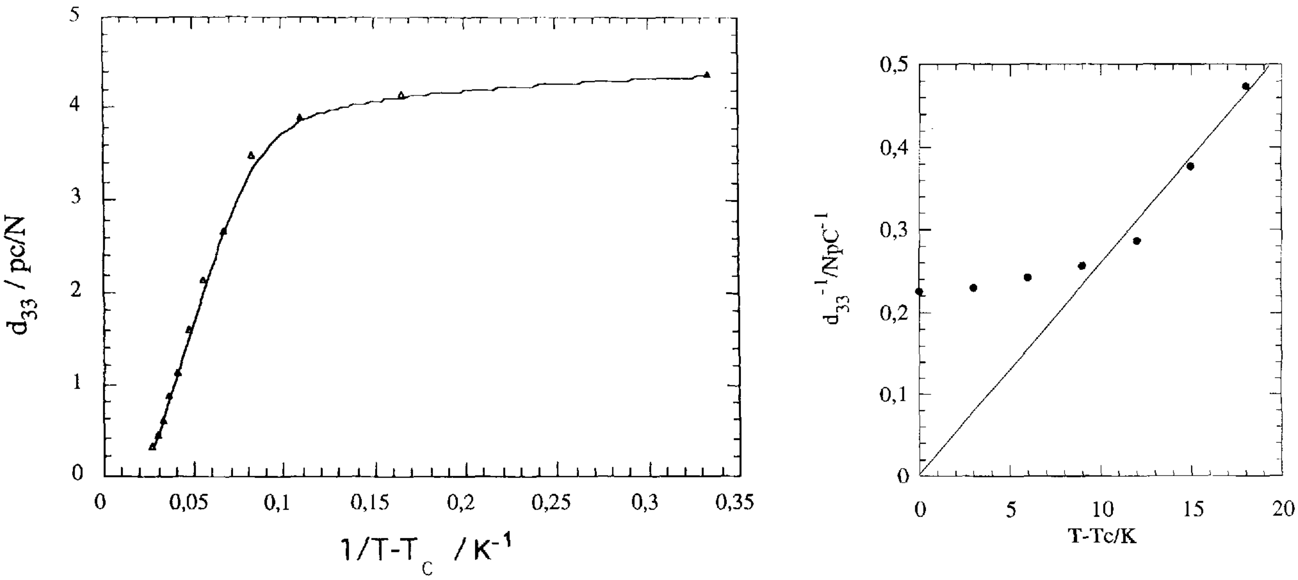

(*a*) (*b*)

Figure 7. (*a*) Temperature dependence of the piezo-coefficient of LC elastomer **2**; (*b*) reciprocal value against reduced temperature (note: only the polar response in the $S_A^*$ phase above 49°C is plotted, data taken from ref. [10]).

ical, electro-optical and mechano-optical properties and opens a fascinating and innovative field of advanced materials design.

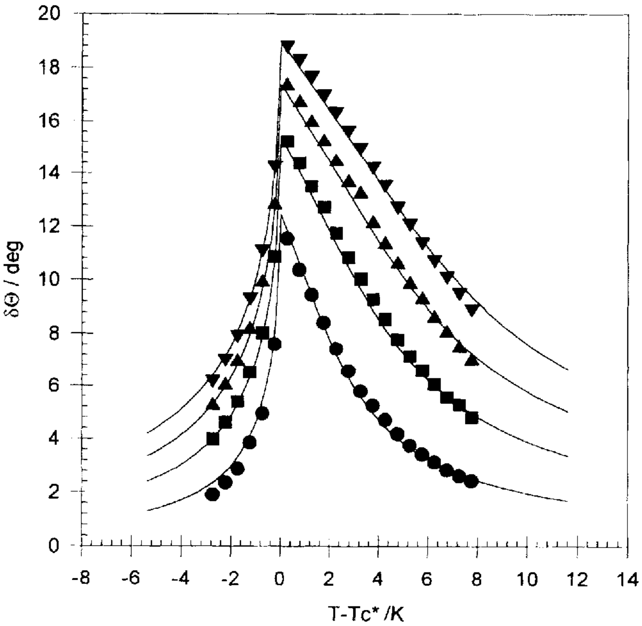

Figure 8. Temperature dependence of the electronic effect. Applied field: (●) 5 MV m$^{-1}$, (■) 10 MV m$^{-1}$, (▲) 15 MV m$^{-1}$, (▼) 20 MV m$^{-1}$.

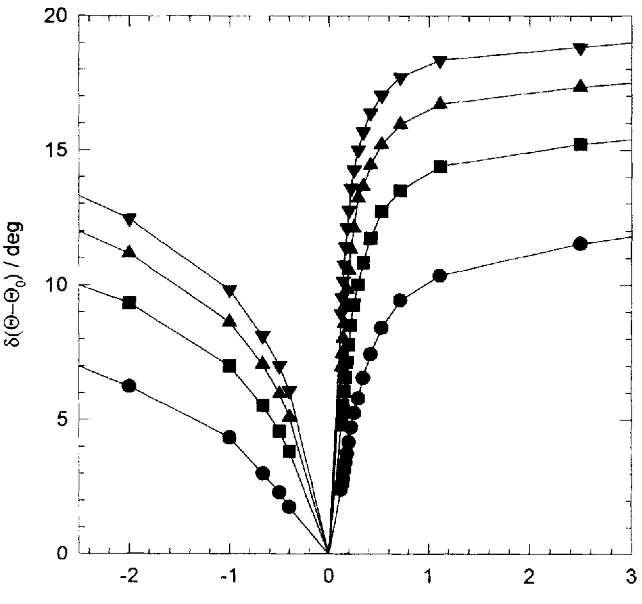

Figure 9. Inverse electroclinic effect. Applied field: (●) 5 MV m$^{-1}$, (■) 10 MV m$^{-1}$, (▲) 15 MV m$^{-1}$, (▼) 20 MV m$^{-1}$.

## References

[1] Treloar, L. R. G., 1975, *The Physics of Rubber Elastics* (Oxford: Clarendon Press).

[2] Noirez, L., Pépy, G., Keller, P., and Benguigui, L., 1991, *J. Phys. II France*, **1**, 821.

[3] Finkelmann, H., Koch, H.-J., and Rehage, G., 1981, *Makromol. Chem. Rapid Commun.*, **2**, 317.

[4] Zentel, R., and Benalia, M., 1987, *Makromol. Chem.*, **188**, 665.

[5] Broer, D. J., Boven, J., Mol, G. N., and Challa, G., 1989, *Makromol. Chem.*, **190**, 2255.

[6] Küpfer, J., and Finkelmann, H., 1991, *Makromol. Chem. Rapid Commun.*, **12**, 717.

[7] Zentel, R., 1986, *Liq. Cryst.*, **1**, 589.

[8] Barnes, N. R., Davis, F. J., and Mitchell, G. R., 1989, *Mol. Cryst. liq. Cryst.*, **168**, 13.

[9] Brehmer, M., Wiesemann, A., Zentel, R., Siemensmeyer, K., and Wagenblast, G., 1993, *Polymer Preprints*, **34**, (**2**), 708.

[10] Brehmer, M., Zentel, R., Wagenblast, G., and Siemensmeyer, K., 1994, *Macromol. Chem. Phys.*, **195**, 1891.

[11] Terentjev, E. M., and Warner, M., 1994, *J. Phys. II*, **4**, 89.

[12] Gießelmann, F., and Zugenmaier, P. (to be published).

[13] P. G. DeGennes and J. Prost, 1993, *The Physics of Liquid Crystals*, 2nd Edn (Oxford: Clarendon Press), p. 529.

[14] Žekš, B., 1984, *Ferroelectrics*, **53**, 33.

[15] Clark, N. A., and Lagerwall, S. T., 1981, in *Ferroelectric Liquid Crystals: Principles, Properties and Applications*, edited by G. T. Taylor and L. A. Shulalov (Philadelphia: Gordon and Breach Science Publishers).

[16] Gießelmann, F., and Zugenmaier, P., 1995, *Phys. Rev. E*, **52**, 2.